

Understanding the Importance of Microphysics and Macrophysics for Warm Rain in Marine Low Clouds. Part II: Heuristic Models of Rain Formation

ROBERT WOOD, TERENCE L. KUBAR, AND DENNIS L. HARTMANN

University of Washington, Seattle, Washington

(Manuscript received 12 January 2009, in final form 30 April 2009)

ABSTRACT

Two simple heuristic model formulations for warm rain formation are introduced and their behavior explored. The first, which is primarily aimed at representing warm rain formation in shallow convective clouds, is a continuous collection model that uses an assumed cloud droplet size distribution consistent with observations as the source of embryonic drizzle drops that are then allowed to fall through a fixed cloud, accreting cloud droplets. The second, which is applicable to steady-state precipitation formation in stratocumulus, is a simple two-moment bulk autoconversion and accretion model in which cloud liquid water is removed by drizzle formation and replenished on an externally specified time scale that reflects the efficacy of turbulent overturning that characterizes stratocumulus.

The models' behavior is shown to be broadly consistent with observations from the A-Train constellation of satellites, allowing the authors to explore reasons for changing model sensitivity to microphysical and macrophysical cloud properties. The models are consistent with one another, and with the observations, in that they demonstrate that the sensitivity of rain rate to cloud droplet concentration N_d (which here represents microphysical influence) is greatest for weakly precipitating clouds (i.e., for low cloud liquid water path and/or high N_d). For the steady-state model, microphysical sensitivity is shown to strongly decrease with the ratio of replenishment to drizzle time scales. Thus, rain from strongly drizzling and/or weakly replenished clouds shows low sensitivity to microphysics. This is essentially because most precipitation in these clouds is forming via accretion rather than autoconversion. For the continuous-collection model, as cloud liquid water content increases, the precipitation rate becomes more strongly controlled by the availability of cloud liquid water than by the initial embryo size or by the cloud droplet size. The models help to explain why warm rain in marine stratocumulus clouds is sensitive to N_d but why precipitation from thicker cumulus clouds appears to be less so.

1. Introduction

A mounting body of observational and modeling evidence suggests that light amounts of warm rain (on the order of 1 mm day^{-1}) falling from low clouds can influence the dynamics and structure of the marine boundary layer (MBL; Paluch and Lenschow 1991; Ackerman et al. 1993; Stevens et al. 1998; Comstock et al. 2005; Savic-Jovicic and Stevens 2008; Xue et al. 2008; Wang and Feingold 2009a,b). This influence can in turn impact the cloud cover and/or thickness and therefore the cloud albedo (e.g., Albrecht 1989; Savic-Jovicic and Stevens 2008). Indeed, over the cold regions of the eastern subtropical and tropical oceans, observations of marine stratocumulus

sheets reveal a striking relationship between the mode of mesoscale cellular convection and the occurrence of drizzle, with open cells frequently associated with strong drizzle and closed cells less frequently so (Stevens et al. 2005; Comstock et al. 2007; Wood et al. 2008).

Over warmer regions of the tropics, cold pools driven by evaporating precipitation also appear to play a fundamental role in the transition from shallow to deep convection (Tompkins 2001; Khairoutdinov and Randall 2006; Kuang and Bretherton 2006). Thus, evidence points to important connections between the formation of precipitation and the organization of shallow convection and ultimately cloud albedo. It is critical that we gain an understanding of the factors controlling the ability of warm clouds to precipitate.

A conventional wisdom, going back to early pioneering studies (e.g., Byers and Hall 1955), is that precipitation occurrence and amount are largely dictated by the macrophysical properties of clouds (e.g., thickness,

Corresponding author address: Dr. Robert Wood, Atmospheric Sciences, Box 351640, University of Washington, Seattle, WA 98195-1640.
E-mail: robwood@atmos.washington.edu

liquid condensate amount, cloud dynamics, etc.). Recently this wisdom is being challenged by evidence suggesting that details of the cloud microphysical properties (e.g., cloud condensation nuclei concentrations, cloud droplet concentration, etc.) may also exert some control over the formation of warm rain. Modeling (e.g., Liou and Ou 1989; Albrecht 1989; Savic-Jovicic and Stevens 2008; Xue et al. 2008; Wang and Feingold 2009a,b) and observational studies (Ferek et al. 2000; Pawlowska and Brenguier 2003; Comstock et al. 2004; vanZanten et al. 2005; Wood 2005a) suggest that N_d may significantly alter the precipitation efficiency of shallow marine clouds. Systematic precipitation closure attempts using multiple case studies demonstrate microphysical control over precipitation rate for stratocumulus clouds (see summary in Geoffroy et al. 2008). However, in the more strongly precipitating trade cumulus regime, such a clear link between N_d and precipitation rate (Nuijens et al. 2009) has not been observed.

Some evidence suggests that the lack of microphysical sensitivity in shallow convection is associated with an increasing dominance of the accretion process over autoconversion as precipitation rates increase (Stevens and Seifert 2008). Because the accretion rate is almost independent of N_d (it depends only on the product of the cloud and rain mixing ratios) whereas autoconversion is strongly sensitive to N_d (Beheng 1994; Khairoutdinov and Kogan 2000; Liu and Daum 2004; Wood 2005b), an increased role of accretion may dampen the sensitivity of precipitation to N_d .

In Part I of this study (Kubar et al. 2009, hereafter Part I) observations from the A-Train satellites were used to determine characteristics of warm rain formation in marine low clouds and to investigate the cloud macrophysical and microphysical factors that influence it. In most regions studied, greater drizzle intensity (higher radar reflectivity) is associated with significant increases in cloud top height and cloud liquid water path (LWP) but with decreases in cloud droplet concentration N_d that are more modest. This is particularly true for regions over the remote oceans that are relatively pristine. In polluted regions off the East Asian coast and over the Gulf of Mexico, higher liquid water contents are required to give the same drizzle intensity as clouds over pristine regions, consistent with a reduction in precipitation efficiency due to higher cloud droplet concentrations.

Here, we introduce two simple heuristic models to attempt to understand the behavior seen in the observations introduced in Part I of this study and to attempt to reconcile the apparently different impacts of microphysics in controlling precipitation amounts in shallow stratocumulus compared with the more strongly precip-

itating trade cumulus regime. Section 2 describes the model physics, section 3 presents some of the essential model behavior, and section 4 describes the observations and how the models are compared with them, with section 5 detailing the results of the comparisons. A discussion of the findings is contained in section 6 and conclusions from the study are given in section 7.

2. Model formulations

a. Continuous collection model

We derive a simple continuous collection (CC) model that determines the precipitation rate at the base of an idealized warm cloud resulting from drops falling and accreting cloud water. It is primarily aimed at reproducing the instantaneous precipitation falling from a cloud that is assumed not to change during the course of the precipitation event. The model inputs are the cloud thickness (or alternatively its liquid water path) and the cloud-top effective radius (or alternatively the cloud droplet concentration).

The assumptions made are detailed below.

1) ASSUMED MACROPHYSICAL CLOUD STRUCTURE

The cloud consists of a layer with a constant specified cloud droplet concentration N_d and a cloud liquid water content ρq_l that increases with height above cloud base z at a specified rate $\rho dq_l/dz = \Gamma$, where q_l is the cloud water mixing ratio and ρ is the air density. The liquid water gradient Γ is given by $\Gamma = f_{ad}\Gamma_{ad}$, where Γ_{ad} is the thermodynamically determined increase for an adiabatic parcel ascent and f_{ad} is the adiabaticity factor. We parameterize $f_{ad} = z_0/(z_0 + z)$ where z_0 is a scaling parameter, set to 500 m, which matches very well with liquid water content observations in warm marine clouds (Rangno and Hobbs 2005) with depths of 1–4 km. Thus, shallow clouds tend to be closer to adiabatic than deeper ones, consistent with arguments for the dilution of entraining plumes (e.g., Bretherton et al. 2004) and with observations (e.g., Rauber et al. 2007).

2) ASSUMED MICROPHYSICAL CLOUD STRUCTURE

The cloud droplet size distribution $n(r)$ is assumed to be a gamma distribution (Austin et al. 1995; Wood 2000) with a spectral width determined as a function of the mean volume radius $r_v = (3\rho q_l/4\pi\rho_w N)^{1/3}$ using the parameterization of Wood (2000) and accounts implicitly for the narrowing of the size distribution due to condensational growth and its broadening (in a fractional sense) due to increased cloud condensation nuclei (CCN) concentration.

TABLE 1. Input and free parameters for the two models in this study.

Parameter type	Model type	
	Continuous collection (CC)	Steady state (SS)
Primary macrophysical	Cloud thickness h (or LWP)	Cloud thickness h (LWP is prognostic)
Primary microphysical	Cloud droplet concentration N_d	Cloud droplet concentration N_d
Others (default values in parentheses)	Adiabaticity scale height z_0 ($z_0 = 500$ m)	Turbulent replenishment time scale τ ($\tau_{\text{rep}} = 1$ h)
	Drizzle drop concentration N_D ($N_D = 100 \text{ L}^{-1}$)	Drizzle drop embryo mass m_{emb} ($m_{\text{emb}} = 4.46 \times 10^{-11} \text{ kg}$)

3) PRECIPITATION EMBRYOS

At the cloud top, a small subset of the largest cloud droplets (specified number concentration N_D) are considered to be precipitation embryos that subsequently are allowed to fall through the cloud layer and grow by coalescing with smaller cloud droplets. Here we specify N_D , which is a free parameter, in accordance with observed concentrations of precipitation drops in warm precipitating clouds and use this to determine the minimum size r_- of the drizzle embryos using

$$\int_{r_-}^{\infty} n(r) dr = N_D. \quad (1)$$

We then use N_D and r_- and the assumed cloud droplet size distribution to determine the mean mass-weighted radius of the embryos R_{emb} ; that is,

$$R_{\text{emb}} = \left[\frac{1}{N_D} \int_{r_-}^{\infty} r^3 n(r) dr \right]^{1/3}. \quad (2)$$

An alternative would be to specify r_- as a free parameter and then use (1) to determine N_D . We experimented with this approach and found that the salient findings were not markedly different. For simplicity, we do not report further on these experiments.

4) COALESCENCE GROWTH OF DRIZZLE DROPS

The drizzle embryos, which are represented by a single-sized embryo with an initial radius R_{emb} , then fall through the depth of the cloud continuously collecting cloud droplets and growing in radius at a rate that is approximately the product of the cloud liquid water content, the collector drop fall speed, and a collection efficiency (Rogers and Yau 1989). The cloud droplets collected are assumed to have a size equal to r_v at that level. The radius growth rate of the falling drizzle drop R with respect to height is taken from the continuous collection model (see, e.g., Rogers and Yau 1989):

$$\frac{dR}{dz} = -\left(1 + \frac{r_v}{R}\right)^2 \left[1 - \frac{v_T(r_v)}{v_T(R)}\right] \frac{\rho q_l E(R, r_v)}{4\rho_w}, \quad (3)$$

where v_T is the terminal velocity of a falling drop, $E(R, r_v)$ is the collection efficiency of the falling drizzle drop and the collected cloud droplets, and ρ_w is the density of liquid water. Terminal velocities for the cloud droplets [$v_T(r_v)$] are determined using the Stokes flow relations given in Pruppacher and Klett (1997), whereas for collector drops we use a power-law relation suitable for drizzle drops (Comstock et al. 2004, detailed below). Collection efficiencies are taken from Hall (1980). The negative sign in (3) indicates that the drizzle drops grow downward. The drops are assumed to be falling in still air.

5) DETERMINING BULK DRIZZLE CHARACTERISTICS

At any level in cloud ($0 < z < h$), the drizzle liquid water mixing ratio $q_{l,D}$ and precipitation rate P and Rayleigh radar reflectivity factor Z are determined using R :

$$q_{l,D} = \frac{4\pi\rho_w}{3\rho} N_D R^3, \quad (4)$$

$$P = \frac{4\pi\rho_w}{3} \alpha_T N_D R^{3+\delta}, \quad (5)$$

$$Z = 2^6 N_D R^6. \quad (6)$$

Here, we use the approximate formulation for the terminal fall speed $v_T(R) = \alpha_T R^\delta$ with $\alpha = 2.2 \times 10^5 \text{ m}^{-0.4} \text{ s}^{-1}$ and $\delta = 1.4$, values taken from (Comstock et al. 2004).

CC model—Free parameters

The key free parameters of the CC model, as shown in Table 1, are the cloud thickness h (or equivalently LWP insofar as it is uniquely related to h) and the cloud droplet concentration N_d . Experimentation shows relatively weak sensitivity of the precipitation characteristics (when expressed as a function of liquid water path) to the choice of the liquid water adiabaticity scaling parameter z_0 . This is because the total condensate through which the collector drop falls is much more important than the details of the vertical organization of the condensate. We use a constant value of $\Gamma_{\text{ad}} = 2 \times 10^{-6} \text{ kg m}^{-4}$.

The cloud-top effective radius r_e^+ , which can be estimated from satellite measurements, is determined

uniquely from the mean volume radius at the top of the cloud r_v^+ , which is a function of cloud-top liquid water content and N_d .

b. Steady-state bulk autoconversion/accretion model

The second model we introduce—the steady-state (SS) model—is a highly simplified model of precipitation formation in a stratiform layer cloud in which there exists (in steady state) a balance between a loss of cloud water through collision–coalescence and its replenishment by assumed turbulent motions that drive the cloud back toward an adiabatic layer. It is primarily designed as a heuristic model to reproduce the equilibrium behavior of precipitation in stratiform boundary layer clouds. The model uses a two-moment bulk microphysical formulation (two moments for cloud and two moments for precipitation), with prognostic equations for the cloud water, precipitation water, and the precipitation drop concentration. The assumptions made are listed below.

1) PROGNOSTIC BULK MICROPHYSICAL EQUATIONS

The cloud consists of a single vertically homogeneous layer of thickness h . The cloud state is characterized by a cloud droplet concentration N_d , which is an external, time-invariant parameter, and a cloud liquid water mixing ratio q_l , which evolves in time. The precipitation is characterized by a rain mass mixing ratio q_r and a rain drop concentration N_D , both of which evolve until a steady state is reached. The following equations describe the evolution of the three prognostic variables:

$$\rho \frac{dq_l}{dt} = \rho \frac{(q_{ad} - q_l)}{\tau_{rep}} - A_c - K_c, \quad (7)$$

$$\rho \frac{dq_r}{dt} = A_c + K_c - S_q, \quad (8)$$

$$\frac{dN_D}{dt} = \frac{A_c}{m_{emb}} - S_N. \quad (9)$$

Here q_{ad} is the adiabatic mean liquid water mixing ratio for the layer (determined as $\frac{1}{2}\Gamma_{ad}h$; see section 2a above), to which q_l relaxes with a replenishment time scale τ_{rep} . The autoconversion rate A_c is a specified function of the cloud state q_l , N_d (see assumption 2 below). The accretion rate is specified as $K_c = \gamma\rho^2q_lq_r$, with $\gamma = 4.7 \text{ m}^3 \text{ kg}^{-1} \text{ s}^{-1}$ as in the formulation of Tripoli and Cotton (1980). Observations suggest that diversity across different accretion rate formulations is modest compared with that across autoconversion rate formulations (Wood 2005b), and we find that our findings are barely altered by using a different formulation (not shown).

The sedimentation rates for rainwater S_q and rain number S_N are specified as $S_q = 2\rho q_r v_{T,q}/h$ and $S_N = 2N_D v_{T,N}/h$ respectively, where $v_{T,q}$ and $v_{T,N}$ are the fall speeds for the third and zeroth moment of the rain size distribution, each of which is specified as a linear function of the rain drop volume radius $r_{v,D} = [3\rho q_r / (4\pi\rho_w N_D)]^{1/3}$ using the parameterization of Khairoutdinov and Kogan (2000). Finally, m_{emb} is the mass of a drizzle drop embryo formed by autoconversion, which we assume to have a radius of $22 \mu\text{m}$, consistent with observations in stratocumulus (Wood 2005b). The results are not highly sensitive to the exact choice of this radius.

2) SENSITIVITY TO AUTOCONVERSION

Available expressions for the autoconversion rate differ markedly in their sensitivities to q_l and N_d (Wood 2005b), so we investigate the sensitivity of our findings to these differences by using a number of different autoconversion parameterizations. We use the formulations of Khairoutdinov and Kogan (2000), Liu and Daum (2004) (as modified by Wood 2005b), Beheng (1994), and Seifert and Beheng (2001); these parameterizations are referred to hereafter as KK, LD, BEH, and SB.

3) STEADY-STATE SOLUTIONS

The model is run with $q_l(t=0) = 0$ until a steady state has been reached.

4) DETERMINING BULK DRIZZLE CHARACTERISTICS

The model precipitation rate, implicitly assumed to be that at the base of the cloud layer, is $P_{CB} = \rho q_r v_{T,q}$. The model estimates a Rayleigh radar reflectivity factor due to precipitation Z from the two moments q_r and N_D by assuming an exponential size distribution truncated at the assumed threshold for cloud and drizzle drop ($r = 20 \mu\text{m}$).

Steady-state model—Free parameters

The free parameters of the steady-state autoconversion and accretion model are the cloud thickness h , the cloud droplet concentration N_d , and the cloud water replenishment time scale τ_{rep} (see Table 1 for values used here). We use a constant value of $\Gamma_{ad} = 2 \times 10^{-6} \text{ kg m}^{-4}$.

3. Model behavior

a. Sensitivity of precipitation rate to LWP and N_d

Before attempting to address the question of how faithfully our two models are able to capture the salient features of the A-Train observations, it is useful to explore some of the essential model behavior.

Figure 1 shows the cloud base precipitation rate P_{CB} as a function of the cloud LWP and the cloud droplet

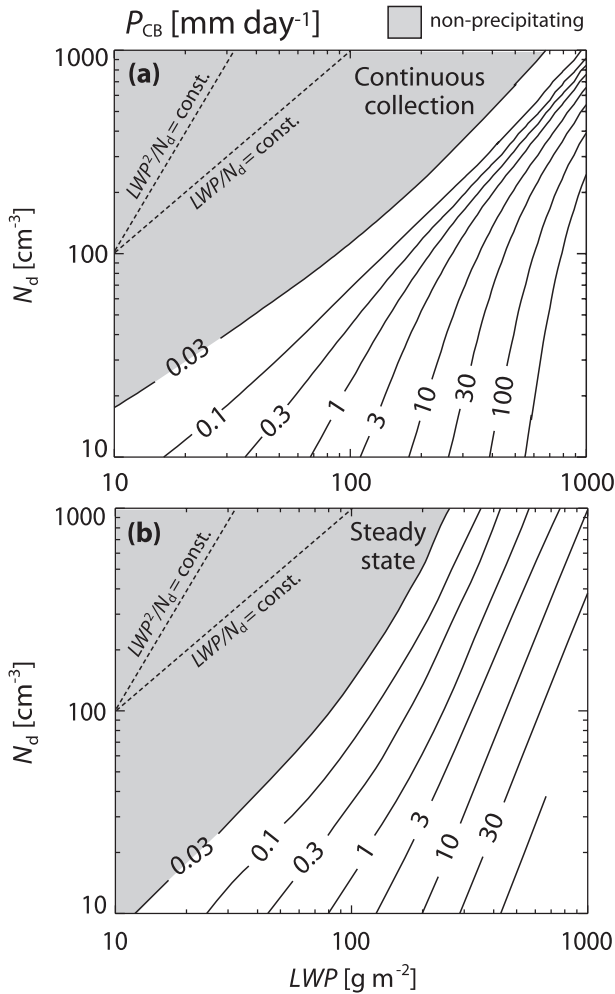


FIG. 1. Cloud base precipitation rate P_{CB} as a function of cloud LWP and cloud droplet concentration N_d for (a) the CC model and (b) the SS model, using the Khairoutdinov and Kogan autoconversion formulation. Model parameters are given in Table 1. The gray area indicates the parameter space where clouds are nonprecipitating (using a threshold of 0.03 mm day^{-1}). Lines (dashed) indicating different relationships between LWP and N_d are presented for reference.

concentration N_d from the CC and SS models (the latter with the Khairoutdinov and Kogan autoconversion parameterization). Both models show that the highest precipitation rates are associated with clouds with high LWP and also with low N_d , and both show similar regions of phase space where P_{CB} is effectively zero. The models are in the best agreement for $N_d < 100 \text{ cm}^{-3}$. At higher N_d there is a significantly stronger dependence of P_{CB} on N_d in the CC model than in the SS model. The Khairoutdinov and Kogan autoconversion parameterization was derived from bin-resolved large-eddy simulation for N_d typical of clean marine conditions (Khairoutdinov and Kogan 2000), with almost all N_d

values below 120 cm^{-3} and so we might not expect it to perform well at high N_d . However, similar discrepancies exist between the CC and SS models at $N_d > 100 \text{ cm}^{-3}$ for the other autoconversion parameterization schemes used in the SS model. Thus, differences in P_{CB} produced by the CC and SS models are not primarily driven by subtleties in the autoconversion parameterizations used.

Both models show a steepening of the P_{CB} isolines (isohyets) as P_{CB} increases (Fig. 1), demonstrating an increase in the relative dependence on LWP compared with N_d at large P_{CB} . We can understand this behavior in the CC model using a minimal analytical CC model (see the appendix), which demonstrates that as LWP increases the key process limiting the rain rate becomes the availability of cloud liquid water to accrete onto growing raindrops rather than the initial size of the precipitation embryos or their efficiency as collector drops to accrete cloud liquid water. However, at high droplet concentrations typical of polluted conditions (N_d of a few hundred per cubic centimeter or more), the initial embryo size can still be an important limiter of precipitation formation even at LWP typical of a few hundred g m^{-2} . Insofar as the CC model is a reasonable replicator of reality, these results have important implications for the sensitivity of warm rain formation to cloud microphysics.

It should be noted however, that the CC model precipitation isolines are much more tightly packed for high LWP and high N_d than those from the SS model. This behavior is more or less reproduced by the minimal CC model (see Fig. A2 and associated discussion in the appendix) and is caused by the extreme sensitivity of the collection efficiency to droplet size for droplets of around $10 \mu\text{m}$ and smaller (see Fig. A1). The SS model does not reproduce this behavior because its bulk autoconversion formulations are not particularly designed to capture this sensitivity. In the application of autoconversion in many models, a threshold function is frequently applied that is usually a function of a characteristic cloud droplet radius (Liu et al. 2005). This is designed to replicate (in most cases somewhat crudely) the strong sensitivity of collection efficiency at small droplet sizes. Because these threshold functions are typically highly arbitrary, used as tuning parameters, and affect a relatively limited portion of the phase space we explore in this study, we do not consider their impacts further here.

b. Sensitivity to model parameterizations

1) CC MODEL

The CC model is sensitive to the number concentration N_D of precipitation embryos (see model assumption 3 in section 2a), which is set equal to 100 L^{-1} , a number toward the upper end of observed concentrations of

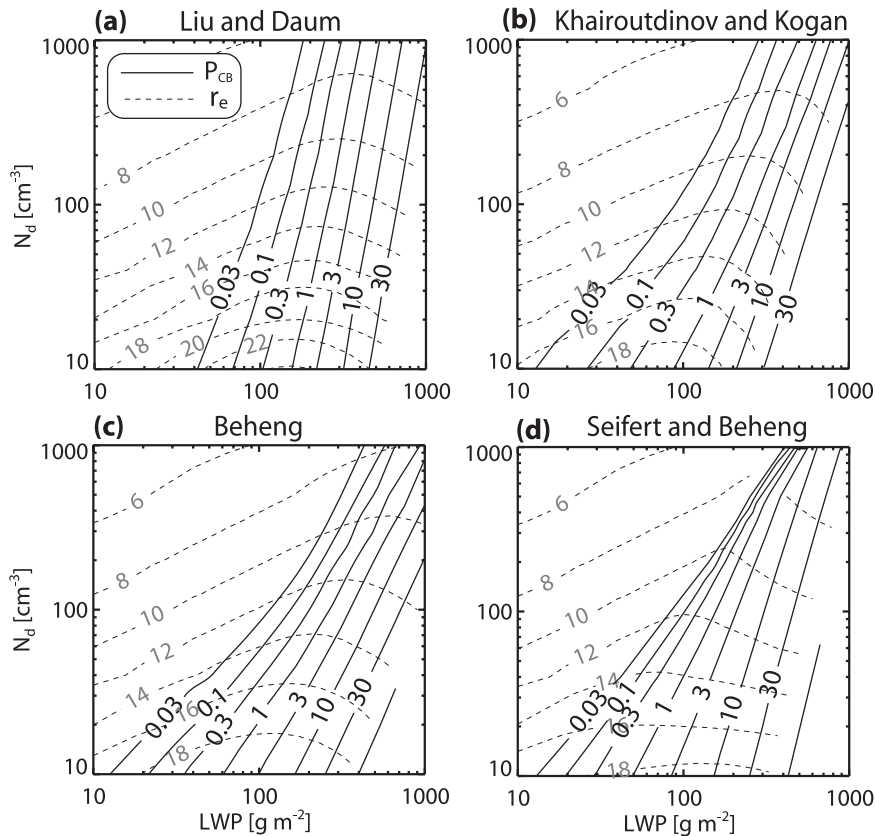


FIG. 2. SS model precipitation rate P_{CB} (solid) and effective radius r_e (dashed) as a function of LWP and N_d for the four autoconversion parameterizations described in the text. Free parameters used in the model are shown in Table 1.

drops with radii larger than $20 \mu\text{m}$ in precipitating warm clouds (Hudson and Svensson 1995; Comstock et al. 2004; Wood 2005a). We find that a doubling of N_D results in an increase of 50%–80% in precipitation rate, an increase that is weaker than linear because a higher N_D is partly compensated by a smaller mass-weighted embryo radius R_{emb} (see model assumption 3 in section 2a). Nevertheless, there is little doubt that the need to specify N_D remains a significant limitation of the CC model.

The CC model precipitation rate is only weakly sensitive to z_0 when expressed as a function of LWP. Increases of only 5%–20% in P_{CB} are found for a given [LWP, N_d] pair as z_0 increases from 250 to 1000 m.

2) SS MODEL

The SS model results display some sensitivity to the autoconversion parameterization used. Figure 2 shows that the greatest fractional sensitivity of precipitation rate to autoconversion parameterization is generally at low values of P_{CB} (i.e., at low LWP and high N_d). For example, at $\text{LWP} = 100 \text{ g m}^{-2}$ and $N_d = 50 \text{ cm}^{-3}$, P_{CB} values are 0.05, 0.15, 0.13, and 0.5 mm day^{-1} (i.e., an

order of magnitude spread) for the four parameterizations (LD, KK, BEH, SB) respectively, whereas at $\text{LWP} = 400 \text{ g m}^{-2}$ and $N_d = 20 \text{ cm}^{-3}$, P_{CB} values are 13, 31, 45, and 55 mm day^{-1} , respectively. For reference, the CC model rates are 0.2 and 38 mm day^{-1} respectively for the low and high LWP cases.

Thus, there is a somewhat weaker sensitivity of P_{CB} to autoconversion parameterization at high P_{CB} . However, more striking is that the sensitivity of P_{CB} to changes in LWP and N_d is much less dependent upon the autoconversion parameterization at high P_{CB} . This can be seen by the spacing and the orientation of the P_{CB} iso-lines in Fig. 2, which are less autoconversion-dependent to the lower right of the panels.

In other words, although the autoconversion impacts the precise value of P_{CB} , the role of the autoconversion parameterization in determining the sensitivity of P_{CB} to changes in, for example, aerosols, is diminished for strongly precipitating clouds. We return to this in the discussion.

The SS model P_{CB} is also sensitive to the cloud liquid water replenishment time scale τ_{rep} , and Fig. 3 shows

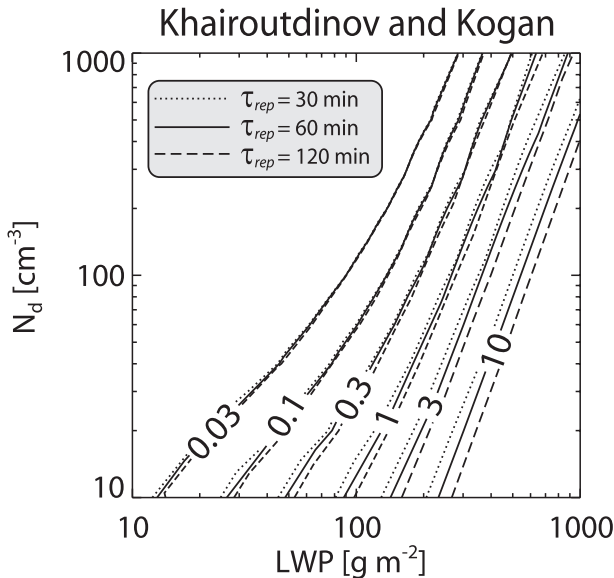


FIG. 3. Sensitivity of the SS model precipitation rate P_{CB} to replenishment time scale τ_{rep} . Contours are shown for values of τ_{rep} equal to 30, 60, and 120 min.

that sensitivity to τ_{rep} is strongest at high P_{CB} . This is because at low P_{CB} the clouds are close to adiabatic because sedimentation is inefficient at removing cloud water. As the precipitation efficiency increases (i.e., the time scale for precipitation removal becomes comparable with τ_{rep}), increasing the replenishment rate of cloud liquid water (decreasing τ_{rep}) permits a larger total rate of conversion of cloud to rain and a larger P_{CB} . However, although Fig. 3 shows that there is sensitivity of the precipitation rate to τ_{rep} , it is primarily LWP and N_d that determine the precipitation sensitivity. The results for the other autoconversion parameterizations are qualitatively very similar (not shown).

We should note that the SS model does not attempt to parameterize the effect of turbulence on recycling of drizzle drops themselves, only the replenishment of the cloud water that feeds the drizzle. The former is known to be important for the formation of the largest drizzle drops in precipitating stratocumulus (Nicholls 1989; Baker 1993; Austin et al. 1995), but including this effect here would add an additional level of complexity that we choose to defer to future study.

4. Comparing the models with observations

a. Observations

How well do our models reproduce behavior seen in nature? To assess this we first examine some previous precipitation closure studies, before turning to observations of radar reflectivity from the *CloudSat* satellite and visible/near-infrared estimates of cloud liquid water path

and collocated cloud droplet concentration from Moderate Resolution Imaging Spectroradiometer (MODIS) on NASA's *Aqua* satellite.

Precipitation closure studies (Pawlowska and Brenguier 2003; Comstock et al. 2004; vanZanten et al. 2005; Wood 2005a; Geoffroy et al. 2008; Brenguier and Wood 2009) attempt to determine the sensitivity of precipitation rate to macrophysical and microphysical cloud properties by exploring numerous case studies spanning a range of different conditions. Currently, systematic exploration is limited to cases in marine stratocumulus, where the precipitation rates are mostly lower than 1 mm day^{-1} , the LWP is 200 g m^{-2} or less, and N_d is $\sim 200 \text{ cm}^{-3}$ or less. In general, these studies all show a strong sensitivity of precipitation rate to cloud liquid water path and a weaker but inverse sensitivity to cloud droplet concentration [see, e.g., Geoffroy et al. (2008) for an integration of the existing studies].

Assuming linearly increasing cloud liquid water content with height in cloud, aircraft closure studies suggest a dependence on $\text{LWP}^{1.5-2}/N_d$, and a ship-based study is more consistent with $(\text{LWP}/N_d)^{1.75}$. Figure 1 shows lines of constant LWP/N_d and LWP^2/N_d , which span the observed range of sensitivity. Both the SS model and CC model isohyets for the region of (LWP, N_d) phase space to which they apply are broadly consistent with the closure studies. Unfortunately, no closure studies exist with which to evaluate the dependencies at higher precipitation rates associated with deeper marine low clouds.

Extensive details regarding the *CloudSat*/MODIS observations and their limitations can be found in Part I of this paper. In this part of the study we attempt to reproduce, using the CC and SS models, the observed dependency of the column maximum radar reflectivity on the cloud LWP and N_d . We use the eight different regions over the subtropical and tropical Pacific Ocean and Gulf of Mexico defined in Part I (see Table 2 here and also Fig. 5 in Part I), together with a region that covers the oceanic region between 30°S and 30°N and 100°E and 70°W .

For each region joint probability distribution functions (PDFs) of LWP and effective droplet concentration¹ (N_{eff}) are constructed from the MODIS retrievals for all the matched *CloudSat*/MODIS data with detectable radar reflectivity and retrieved cloud properties. A selection of statistical properties is shown in Table 2, which are discussed in some detail in Part I. In Part I we demonstrated that the radar reflectivity (which for reflectivities greater than -15 dBZ is inferred to be precipitation)

¹ The effective droplet concentration N_{eff} is retrieved from the MODIS estimates of cloud optical thickness and cloud-top effective radius under the assumption that the cloud liquid water content follows an adiabatic vertical profile. See Part I for further details.

TABLE 2. Regions used for observational/model comparison in this study, together with parameters indicating the macrophysical and microphysical cloud properties determined using the A-Train data described fully in Part I. Only clouds over open ocean are included. Bold numbers represent the maximum value among all regions, and italics represent minimum values. All numerical values represent median values for the region.

Region	Lat	Lon	Cloud-top height (km)	LWP (g m^{-2})	r_e^+ (μm)	N_{eff} (cm^{-3})
Northeast Pacific	15–30°N	150°E–130°W	2.0	177	16.7	44
Far northeast Pacific	15–30°N	105–125°W	1.4	138	13.9	71
Gulf of Mexico	20–30°N	70–100°W	2.3	250	12.2	127
Asian coast	15–30°N	100–130°E	2.2	264	<i>11.5</i>	159
Southeast Pacific	15–30°S	90–150°W	2.1	161	18.0	33
Far southeast Pacific	0–30°S	70–80°W	1.3	108	13.2	72
	5–15°N	140°E–140°W				
Deep convective	5–15°S	150°E–130°W	2.7	216	17.1	44
Equatorial cold tongue	5°S–5°N	85–130°W	1.7	155	14.6	61

scales with both LWP and N_{eff} , which we refer to here as our macrophysical and microphysical cloud properties. Here, we will ask how faithfully our heuristic models can reproduce the general characteristics of the radar reflectivity as a function of LWP and N_{eff} .

b. Treatment of CC model output for comparison with observations

For the CC model the precipitation rate and reflectivity factor due to precipitation maximize at the cloud base. The radar reflectivity factor at the cloud base Z_{cb} is corrected for Mie scattering at 94 GHz (the wavelength of the *CloudSat* radar) using the approach of Comstock et al. (2004). To estimate the Mie correction, we assume that the drizzle drop radius R represents the mean volume radius of an assumed exponential drizzle size distribution, for which a Mie correction is derived from the Mie routine in Bohren and Huffman (1998). The Mie correction is applied to the column maximum reflectivity, which is constrained in the model to be at the cloud base. For a radar reflectivity factor of 7.5 dBZ (which corresponds to a rain rate of approximately 2 mm h^{-1}), we found that the Mie correction is approximately 2.5 dBZ and increases by approximately 1 dBZ for each 2 dBZ increase in Z_{cb} . Because few of the shallow clouds in this study produce rain significantly heavier than this, the Mie correction for warm rain does not have a major impact.

To further facilitate comparison with *CloudSat*, the Mie-corrected model reflectivity is then corrected for two-way attenuation at 94 GHz given the cloud liquid water path using a two-way attenuation coefficient of $8.4 \text{ dBZ} (1000 \text{ g m}^{-2})^{-1}$ (Lhermitte 1990). This correction becomes significant for high LWP, but for most LWP values here (typically up to a few hundred g m^{-2}) it is relatively modest. Both the Mie scattering and attenuation corrections only affect the statistics for the subset of model clouds that is precipitating most strongly. The corrected model reflectivity is given the symbol Z_{model} .

The cloud particles that in the model are the initial source of the precipitation also scatter and frequently dominate the reflectivity signature when the precipitation rates are lower than a few tenths of a millimeter per day. The assumed gamma distribution is used to determine the cloud reflectivity, which is largest at cloud top. Because of this and because Mie scattering is not important for cloud drops, the reflectivity from cloud drops does not require corrections. Finally, the model's column maximum reflectivity is determined as the maximum of that due to cloud and precipitation.

We should note here that in the CC model the reflectivity from cloud droplets only exceeds that due to precipitation for cases with very light amounts of precipitation (less than a few tenths of a millimeter per day or reflectivities lower than -10 dBZ). Such rates are not likely to have a significant dynamical impact and so for most relevant precipitation rates the radar reflectivity is primarily providing information about precipitation and not cloud.

c. Treatment of SS model data

The SS model radar reflectivity due to precipitation (which is implicitly assumed to maximize at cloud base) is corrected for Mie scattering and attenuation as a function of LWP in the same way as for the CC model. The mean volume radius of the drizzle drops $r_{v,D}$ is used to determine a Mie scattering correction, and the LWP is used to determine the attenuation.

The cloud contribution to the reflectivity (which is assumed to maximize at cloud top despite the model lacking an explicit vertical dimension) is determined by assuming a gamma distribution for the cloud droplet size distribution, with inputs q_l , N_d , and a parameterized spectral width in exactly the same manner as for the CC model (see assumption 2 in section 2a above). The reflectivity from cloud droplets does not require correction for Mie scattering.

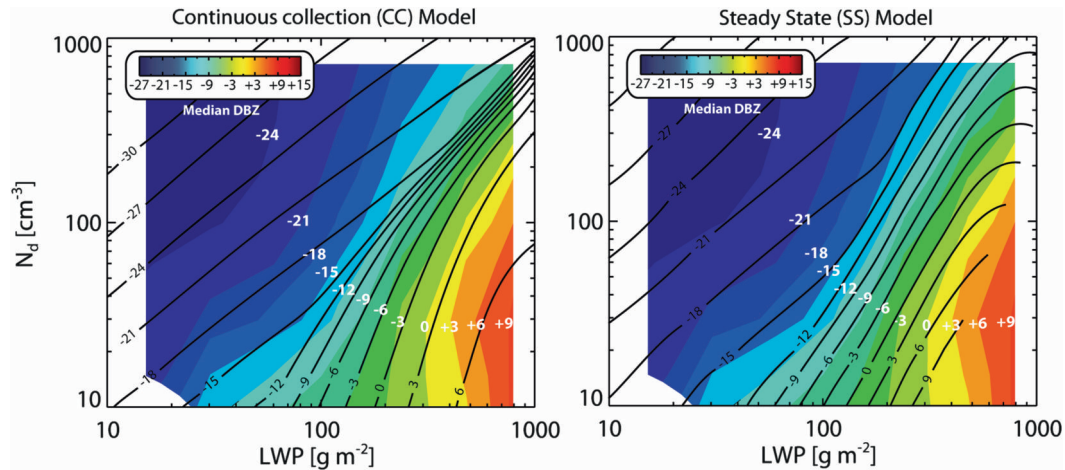


FIG. 4. Cloud-base 94-GHz radar reflectivity (solid black lines) from (a) the CC model and (b) the SS model with the KK autoconversion overlaid on A-Train data (colors, with white labels) as a function of the cloud LWP and cloud droplet concentration N_d . For the observations the adiabatic droplet concentration N_{eff} is used. Model inputs are corrected as described in section 4c.

d. Comparison with A-Train data

The CC model is run for $10 < \text{LWP} < 1000 \text{ g m}^{-2}$ and $10 < N_d < 1000 \text{ cm}^{-3}$. The SS model is run for $100 < h < 3000 \text{ m}$, which ensures LWP in the range of $10\text{--}1000 \text{ g m}^{-2}$, and $10 < N_d < 1000 \text{ cm}^{-3}$. We also use the observationally derived joint PDFs of LWP and N_{eff} to determine statistics of the population of clouds in each of our eight focus regions.

To ensure consistency with the observations, which assume adiabatic N_{eff} , the CC model receives a value of N_d corrected for the subadiabatic nature of the assumed model clouds. This is done by determining, for each value of LWP, a cloud thickness that is consistent with the assumed vertical liquid water structure (see assumption 1 in section 2a above). This cloud thickness is then used to estimate the cloud top adiabaticity factor, and this is used to correct N_d . This ensures consistency in the assumed vertical structure between the CC model and the observations. No such correction is made to the SS model because the adiabaticity is an intrinsic model variable.

The statistics we determine from the observations and model are

- (i) the fraction of observed clouds that are precipitating (i.e., have a column maximum corrected reflectivity $Z_{\text{model}} > -15 \text{ dBZ}$);
- (ii) the fraction of clouds with moderate drizzle (corrected reflectivity $Z_{\text{model}} > 0 \text{ dBZ}$);
- (iii) the fraction of clouds with heavy drizzle ($Z_{\text{model}} > 7.5 \text{ dBZ}$);
- (iv) the median reflectivity of all clouds; and
- (v) the median reflectivity of precipitating ($Z_{\text{model}} > -15 \text{ dBZ}$) clouds.

The observed values of (i)–(v) are presented by region in Table 1 of Part I of this study.

Given the Z – R relationship of Comstock et al. (2004), and taking into account the attenuation/Mie corrections appropriate for 94 GHz, a cloud base reflectivity of -15 dBZ corresponds to approximately $0.25\text{--}0.5 \text{ mm day}^{-1}$, whereas 0 dBZ corresponds to $\sim 2\text{--}5 \text{ mm day}^{-1}$ and 7.5 dBZ corresponds to $\sim 20\text{--}40 \text{ mm day}^{-1}$, but we should caution that the attenuation and Mie corrections do upset the uniqueness of the relationship between reflectivity at 94 GHz and rain rate, especially for the heaviest precipitation rates explored in this study. For more accurate study of these rates it would be preferable to use an attenuation-based retrieval such as in Haynes et al. (2009).

5. Comparison results

a. Comparison in the LWP, N_{eff} plane

Figure 4 shows the column maximum 94-GHz radar reflectivity as a function of LWP and N_d from the continuous collection model and for the entire set of A-Train observations within $30^\circ\text{S}\text{--}30^\circ\text{N}$, $100^\circ\text{E}\text{--}70^\circ\text{W}$. In general, both models reproduce critical aspects of the observations with some fidelity. Especially good is the ability to reproduce the threshold between precipitating and nonprecipitating clouds (i.e., the -15-dBZ contour), although the CC model is less skillful at reproducing the observed dBZ structure at high values of LWP and N_{eff} than is the SS model. Both models quite successfully capture the broad change in contour slope as the clouds transition from nonprecipitating to precipitating.

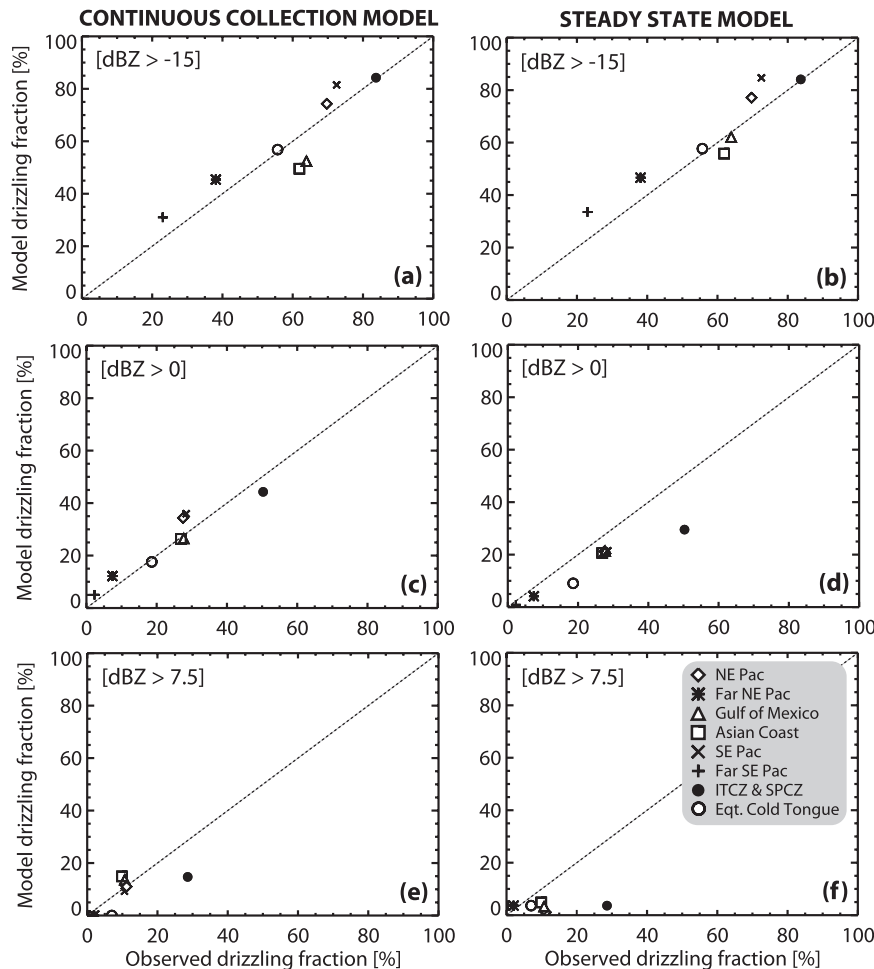


FIG. 5. Comparison of the (left) CC and (right) SS models with observed fraction of clouds with reflectivities greater than (a),(b) -15 , (c),(d) 0 , and (e),(f) 7.5 dBZ for the eight regions given in Table 2. The KK autoconversion parameterization is used in the SS model.

The CC model appears to be more successful than the SS model at capturing the weakening microphysical dependency at high P_{CB} that is seen in the observations and reproduced well by the CC model. However, a comparison of Figs. 1 and 4 suggests that this reflects a different relationship between P_{CB} and Z in the SS model than in the CC model because P_{CB} isolines in the SS model do become more vertical at increased P_{CB} even though the reflectivity isolines do not. However, the P_{CB} isolines in the CC model at high LWP and low N_d are still steeper than the SS model for all autoconversion parameterizations other than SB (see Fig. 2).

b. Comparison of precipitation characteristics by region

For each of the eight regions described in Table 2 we use the observed joint PDF of LWP and N_{eff} to produce model estimates of the metrics introduced in section 4d.

These are compared with the observed values in Figs. 5 and 6. In general, both models successfully reproduce the fraction of observed/screened² clouds that are precipitating (those with reflectivities > -15 dBZ), and also those with $\text{dBZ} > 0$ (moderate drizzle). Thus, to a good degree, both models can determine important characteristics about the distribution of light and moderate drizzle for warm, relatively homogeneous clouds given their LWP and cloud droplet concentration.

However, the models cannot accurately reproduce the fraction of clouds with heavy drizzle ($\text{dBZ} > 7.5$),

² We should note that the observed drizzling fraction reported here should not be confused with the fraction of *all* clouds that are drizzling; rather, it is the fraction of clouds selected as being detectable by both *CloudSat* and MODIS, and being appropriately screened as being optically thick and relatively homogeneous as detailed in Part I.

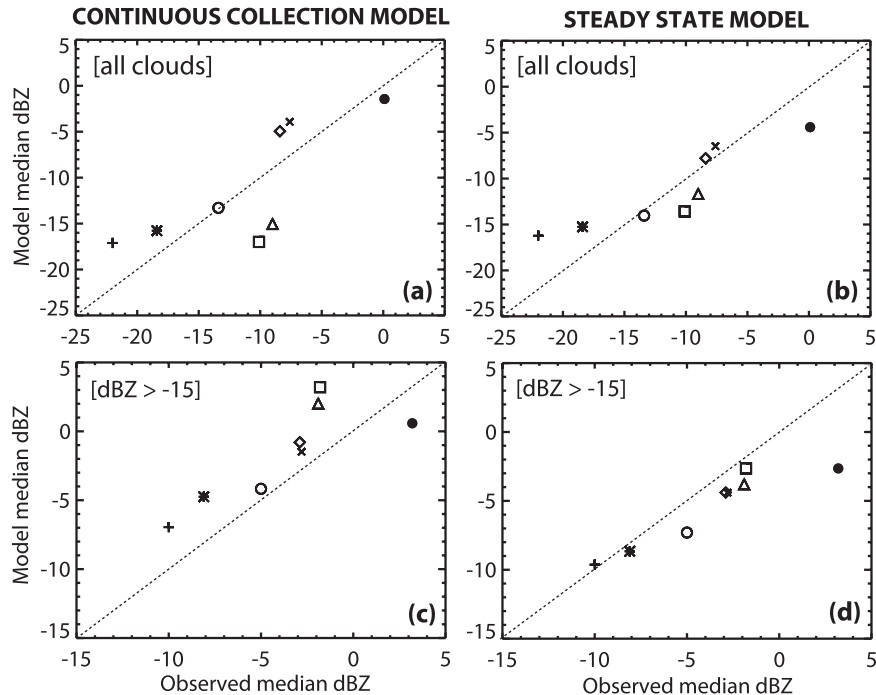


FIG. 6. Comparison of the (left) CC and (right) SS models with observed median 94-GHz reflectivity for (a),(b) all clouds and (c),(d) clouds with reflectivities greater than -15 dBZ for the eight regions given in Table 2. Symbols are as in Fig. 5.

although the CC model displays some skill. This is perhaps not surprising for the SS model given that it is primarily designed to simulate precipitation in overturning stratocumulus clouds, which rarely exhibit precipitation rates greater than 20 mm day^{-1} (Comstock et al. 2004).

It is interesting that the observations show good relationships between the fraction with moderate drizzle and the fraction with any drizzle, and between the fraction with heavy drizzle and that with moderate drizzle (Fig. 7) for the observations and for the CC model. The observed relationships are reproduced fairly well assuming that the distribution of reflectivity in each region is lognormal with a fixed geometrical standard deviation of 14 dBZ (and a variable mean). It is not known whether there is any fundamental significance to the approximately constant standard deviation, but it implies that the spread of precipitation rates (in a fractional sense) in a given region is fairly universal despite considerable differences in the mean precipitation rate. The CC model is able to capture the essence of these relationships with some skill.

The models also perform reasonably well in reproducing the median reflectivities for the different regions (Fig. 6). However, both models underestimate the precipitating fraction ($> -15 \text{ dBZ}$) and the median reflectivity (especially the CC model) for the Asian coast

and Gulf of Mexico regions, which are the two regions with the highest median N_{eff} and LWP. For the CC model, this could have been anticipated given the relatively poor comparison of the model and observed reflectivity structure in the $(\text{LWP}, N_{\text{eff}})$ plane for high LWP and N_{eff} (see the previous section and Fig. 4). It is shown later (Fig. A3; see appendix) that this is the region of phase space where the characteristic droplet radii are around $10 \mu\text{m}$ or smaller, the approximate size at which the collection efficiency changes rapidly with droplet size (e.g., Rogers and Yau 1989). This certainly explains the strong sensitivity of P_{CB} to droplet size in this region for the CC model. The SS model also underestimates the median reflectivity for the ITCZ/SPCZ region, which may reflect its unsuitability for predicting precipitation in strongly drizzling cumuliform clouds.

6. Discussion

a. Sensitivity of warm rain to microphysics and macrophysics

We have seen that the observed distribution of radar reflectivity and its dependence on cloud macrophysical and microphysical properties can be reproduced with some skill using the simple heuristic models presented here. It thus gives us some confidence that we can use the model to infer aspects of the sensitivity of warm rain

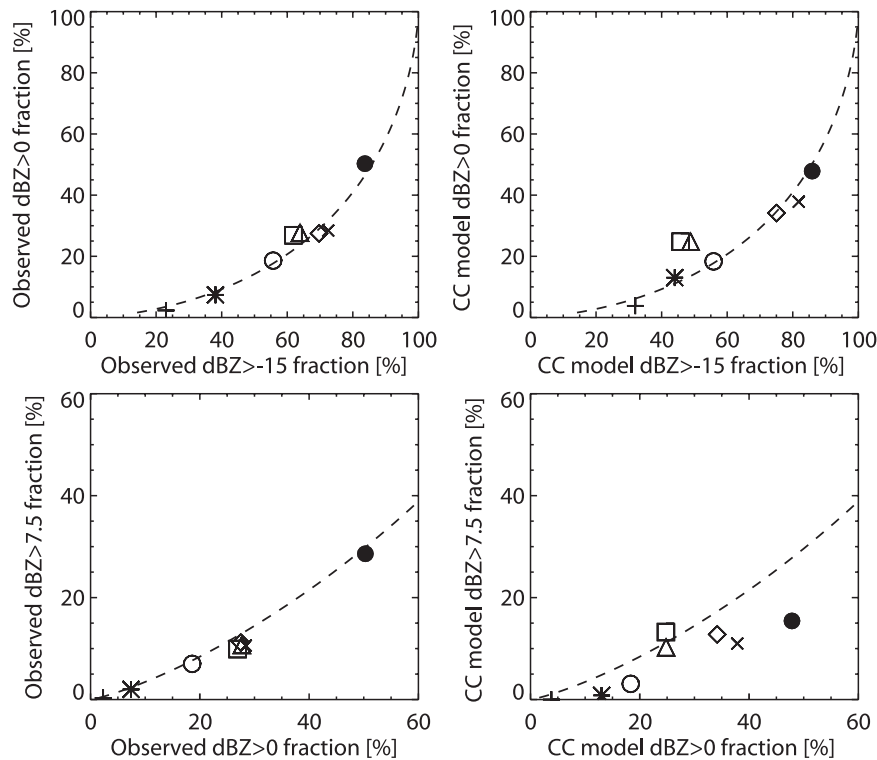


FIG. 7. Relationship (a),(b) between fraction with moderate and all drizzle and (c),(d) between fraction with heavy and moderate drizzle for (left) observations and (right) the CC model for the eight regions given in Table 2. Symbols are as in Fig. 5. The dashed line assumes that in all regions the reflectivity values are distributed lognormally with a fixed geometrical standard deviation of 14 dBZ.

to changes in macrophysical and microphysical cloud properties.

In Fig. 8 we show, for the CC model, the sensitivity of the distribution of reflectivity in each region to an across-the-board increase of 50% in LWP and a 50% decrease in N_{eff} . The behavior of the SS model (not shown) is very similar. Increased LWP results in a shift to the right of the reflectivity PDFs by a substantial amount (roughly 4–5 dBZ, equivalent to around a factor of 2.5–3 increase in reflectivity), whereas the reduction in N_{eff} induces significantly more modest increases in reflectivity. Further, the microphysical sensitivity decreases as the reflectivity increases (from 1–2 dBZ around 0 dBZ to less than 1 dBZ at 5–10 dBZ), consistent with the behavior seen in Fig. 4; this can be explained theoretically (see appendix) as being due to a shift to an accretion-limited regime at high reflectivity. Note that a shift of $10 \log_{10}(1.5) = 1.76$ dBZ is equivalent to a 50% increase in reflectivity.

To confirm that these results are not strongly dependent upon our assumptions about the reflectivity–rain rate relationship, we show a similar plot for the modeled cloud base precipitation rate P_{CB} distributions for the

northeast Pacific region (Fig. 9). At high precipitation rates, the sensitivity of P_{CB} to changes in LWP is much greater than to changes in N_{eff} . This behavior is repeated for the other regions (not shown).

These model results, when taken together with the observed tendency for the reflectivity to become more strongly dependent on LWP as the reflectivity increases (Fig. 4), suggest a markedly diminished ability for cloud microphysics to influence precipitation rates in clouds that are dominated by accretion. Moreover, the ability to unequivocally attribute observed variability in precipitation rates to microphysical changes will therefore be more difficult for clouds with higher precipitation rates. This finding largely explains why, although there is strong evidence for N_d -limited precipitation in drizzling stratocumulus (Pawlowska and Brenguier 2003; Comstock et al. 2004; vanZanten et al. 2005; Wood 2005a; Geoffroy et al. 2008), there is no such evidence for substantial N_d limitation of precipitation in clouds with markedly greater liquid water paths than those found in stratocumulus (Levin and Cotton 2008). Existing observational studies supporting such microphysical impacts are largely flawed in part because they have

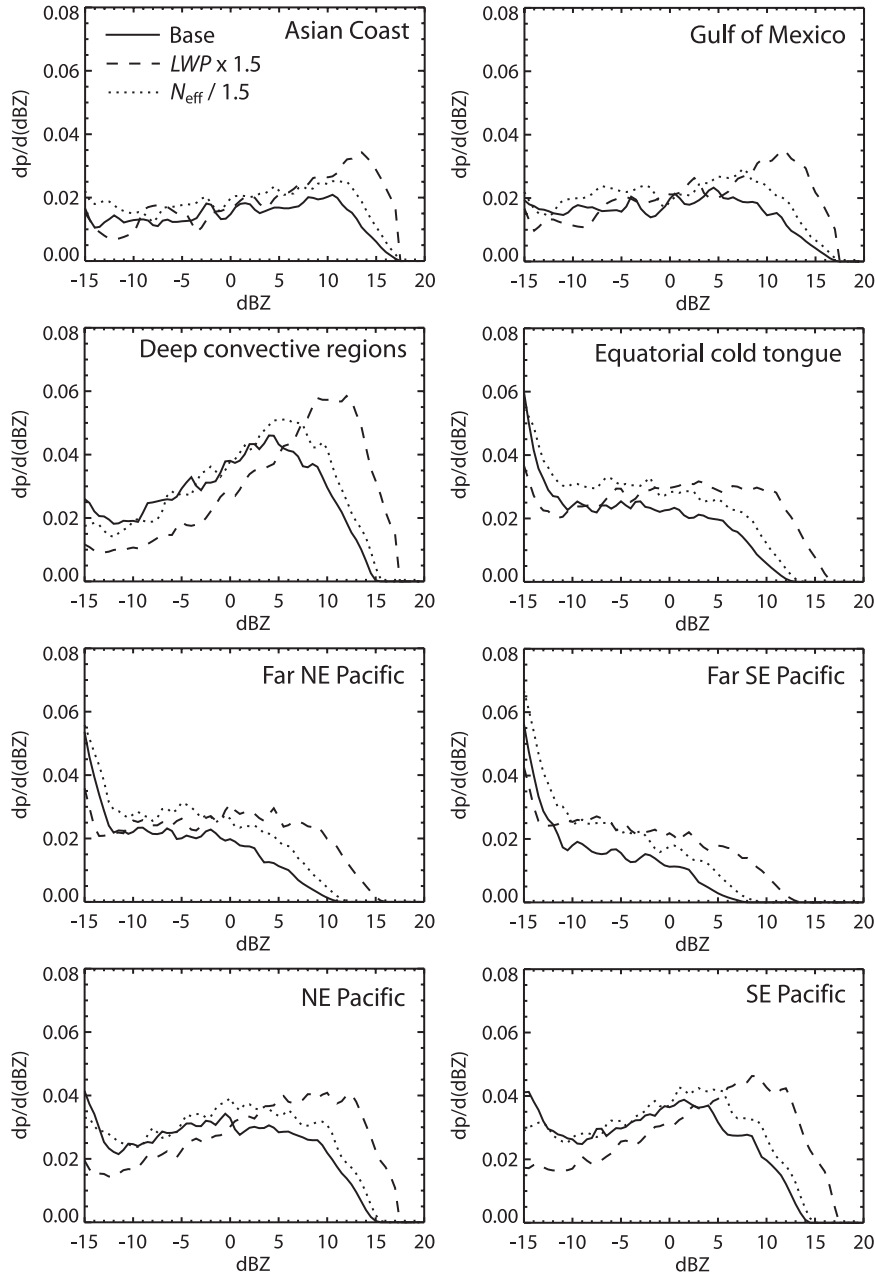


FIG. 8. Distribution of the reflectivity values from the CC model for the eight regions given in Table 2. In each panel are shown the distribution using the observed joint PDF of LWP and N_{eff} (solid) together with the distributions obtained by increasing LWP values by 50% (dashed) and by decreasing N_{eff} by 50% (dotted).

inferred precipitation occurrence from measures such as cloud-top effective radius (see Part I of this study) that have little direct connection to precipitation rate.

b. Steady-state precipitation

For the steady-state model, in which a balance is reached between loss of cloud water by conversion to drizzle and replenishment via turbulent updrafts (time

scale τ_{rep} ; see section 2b), we can define an additional time scale τ_{driz} for the conversion of cloud to drizzle:

$$\tau_{driz} = \frac{\rho q_l}{A_c + K_c} \tag{10}$$

A remarkable behavior of the steady-state model is that the microphysical susceptibility of the cloud base

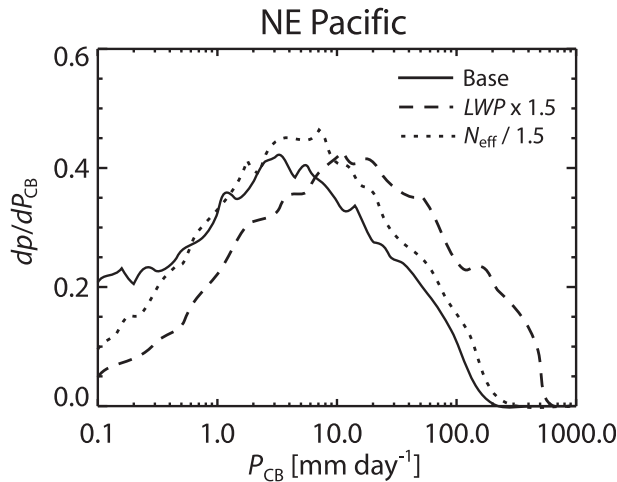


FIG. 9. As in Fig. 8, but showing the distributions of the cloud base precipitation rate P_{CB} from the CC model for the northeast Pacific region (see Table 2).

precipitation rate $S = d \ln P_{CB} / d \ln N_d$ is very strongly related to the ratio of the replenishment to depletion time scales τ_{rep} / τ_{driz} . We examine S for model inputs spanning the $[LWP, N_d]$ phase space shown in Fig. 2, with τ_{rep} spanning 60 to 240 min, and with different autoconversion parameterizations. Figure 10 shows S normalized by the sensitivity of the autoconversion parameterization to changes in N_d (i.e., $\beta = d \ln A_c / d \ln N_d$) as a function of τ_{rep} / τ_{driz} and with this we find that S/β is almost independent of the autoconversion parameterization.

What this tells us is that clouds in steady state with high precipitation efficiency (low τ_{driz}) and/or slow replenishment (high τ_{rep}) have a lower sensitivity to N_d than those with lower precipitation efficiency and/or rapid replenishment. Observations in stratocumulus clouds (Wood 2005a) suggest that replenishment time scales for liquid water in stratocumulus may be a few times the eddy turnover time scale, or around 1–2 h. This is consistent with the lifetimes of mesoscale drizzle cells that frequently dominate the dynamics of these clouds (Comstock et al. 2007). Given that typical liquid water contents in stratocumuli are $\sim 0.5 \text{ g kg}^{-1}$, and that $A_c + K_c$ is on the order of $5 \times 10^{-9} - 5 \times 10^{-8} \text{ kg m}^{-3} \text{ s}^{-1}$ (for precipitation rates of the order of $0.5 - 5 \text{ mm day}^{-1}$), this would put τ_{driz} in the range $10^4 - 10^5 \text{ s}$ and S/β in the range 0.2–0.8. Even drizzling stratocumulus clouds may therefore exhibit a sensitivity to N_d that is substantially weaker than the sensitivity of autoconversion itself. This may explain why precipitation closure observations in stratocumulus show sensitivities to N_d at the lower end of those in most autoconversion parameterizations.

The reasons for this behavior are again consistent with the increased importance of accretion as the precipita-

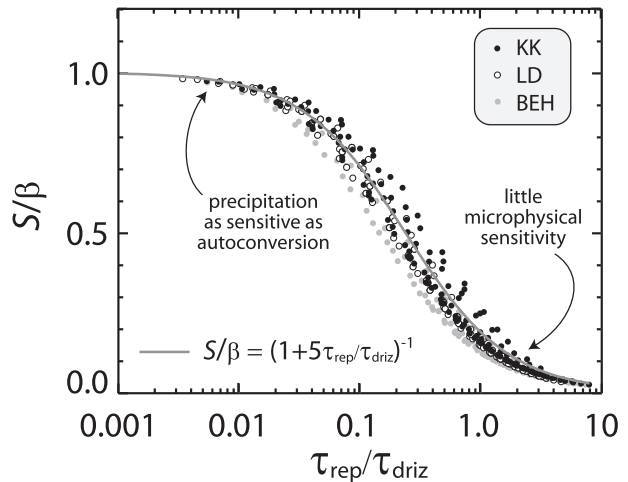


FIG. 10. Fractional sensitivity, for the SS model, of the cloud base precipitation rate to cloud droplet concentration $S = d \ln P_{CB} / d \ln N_d$ normalized with the autoconversion sensitivity β as a function of the ratio of the replenishment to drizzle time scales τ_{rep} / τ_{driz} . Each point represents a *separate* combination of the cloud thickness ($100 < h < 3000 \text{ m}$), droplet concentration ($10 < N_d < 1000 \text{ cm}^{-3}$), τ_{rep} ($30 < \tau_{rep} < 240 \text{ min}$), and the different colors are for different autoconversion parameterizations. For reference, β is -1.79 , -1.0 , and -3.3 for the KK, LD, and BEH autoconversion parameterizations, respectively. The SB parameterization is not included in this plot because the autoconversion rate also depends on the drizzle LWC for this model and so a single value of β cannot readily be defined. The gray line is the arbitrary fit through the data using the function $S/\beta = (1 + 5\tau_{rep}/\tau_{driz})^{-1}$.

tion becomes more efficient at depleting cloud liquid water. In this way the behavior of the SS model is generally consistent with the behavior of the CC model.

c. Representation in large-scale models

Climate models generally show second aerosol indirect effects (AIEs) that are of comparable magnitude to the first AIE (Lohmann and Feichter 2005). This suggests that climate model precipitation is sensitive to cloud microphysical changes induced by increasing aerosol concentrations. Given that the representation of precipitation in climate models is at least as detailed as the steady-state model used here, is it necessary to be concerned about how climate models treat warm rain?

One of the key assumptions in the steady-state model is that precipitation is treated prognostically, whereas in most climate models the longer time steps required render a diagnostic formulation more efficient (e.g., Ghan and Easter 1992). Posselt and Lohmann (2008) show that a prognostic treatment of precipitation increases the relative contribution to precipitation from accretion compared with autoconversion in weakly precipitating clouds. Given that this appears from our model results to be a critical determinant of the sensitivity of

precipitation to cloud microphysics, it may be plausible to hypothesize that diagnostic treatment of warm rain formation in climate models will overestimate the microphysical sensitivity and therefore the second AIE. Further work is required to establish if this is a pathological problem for climate models.

7. Conclusions

In this study, we have attempted to reproduce some of the salient observational results detailed in Part I of this study. These observations, for which important new data from the *CloudSat* satellite is combined with visible/near-IR data from MODIS, demonstrate that the radar reflectivity in precipitating low clouds is influenced both by variability in macrophysical quantities like cloud liquid water path and by microphysical quantities such as the estimated cloud droplet concentration N_{eff} . The observations demonstrate that for clouds with higher reflectivities, the reflectivity is more sensitive to LWP than to N_{eff} . This general tendency is reproduced well by a continuous collection (CC) model of precipitation formation and can be explained by the increasing importance of accretion in controlling the precipitation amount when the precipitation rate is larger than a few millimeters per day.

The general behavior of the observations is replicated using a minimal analytical CC model that aids understanding. Because accretion is largely controlled by the availability of liquid water and is not strongly limited by reduced collection efficiency, this leads to a weakened dependence of precipitation on N_{eff} at high LWP in the accretion-dominated regime. Quantitatively similar behavior is obtained in a bulk microphysical steady-state precipitation model, but there is strong quantitative sensitivity to the choice of autoconversion parameterization.

Finally, the observations suggest that the influence of anthropogenic aerosols (through their ability to act as CCN and influence the cloud droplet concentration) on warm rain is likely to be a strong function of the cloud microphysical and macrophysical state of the clouds into which the aerosols are being ingested. In other words, the susceptibility of warm rain to microphysical changes will likely depend on the type of clouds and therefore on the meteorological regime. It will be useful in future observational and modeling studies to examine this susceptibility as a function of the liquid water path and the cloud droplet concentration.

Acknowledgments. The corresponding author wishes to thank Marcia Baker, Bjorn Stevens, and Axel Seifert for discussions from which the ideas in this paper emanate. The work was supported in part by NASA Grants

NNG05GA19G and NNX08AG91G and a subcontract from the Jet Propulsion Laboratory.

APPENDIX

Minimal CC Model

The form of the relationship of LWP, N_d , and P_{CB} in the CC model is strongly controlled by the dependence of the collection efficiency on the collector drop size. To demonstrate this, a minimal model is constructed that simplifies the warm rain model into an analytical form.

We begin with (3) and retain the R dependence only through the collection efficiency, that is, $E(R, r_v)$. This is reasonable since $\eta \equiv (1 + r_v/R)^2[1 - v_T(r_v)/v_T(R)]$ does not vary strongly with r_v/R , whereas the collection efficiency drops dramatically for small droplets. We set $\eta = 1.2$, and assume a constant value of r_v through the cloud layer. We choose r_v as the liquid water weighted mean value of r_v for the cloud layer. It can be shown that this is $6/7$ times the value at the cloud top r_v^+ for clouds in which liquid water increases linearly with height.

We then integrate (3) from cloud top to cloud base:

$$\int_{R_{\text{emb}}}^{R_{\text{CB}}} E^{-1}(R, r_v) dR = \frac{\eta \text{LWP}}{4\rho_w}. \quad (\text{A1})$$

We then parameterize $E^{-1}(R, r)$, which can be thought of as a collection inhibition factor, as the product of a function depending upon the collector drop radius R and a function depending on the collected drop radius r_v ; that is,

$$E^{-1}(R, r) = Q_r Q_R \approx \left[1 + \left(\frac{a}{R} \right)^5 \right] \left[1 + \left(\frac{b}{r} \right)^4 \right], \quad (\text{A2})$$

with $a = 30.6 \mu\text{m}$ and $b = 6.27 \mu\text{m}$. Figure A1 shows $E^{-1}(R, r)$ from Hall (1980) and from (A2). The parameterization captures the inhibition of coalescence for small values of the collected drop and particularly the collector drop. With the parameterization (A1) becomes

$$\left[R - \frac{a^5}{4} R^{-4} \right]_{R_{\text{emb}}}^{R_{\text{CB}}} = \frac{\eta \text{LWP}}{4\rho_w [1 + (b/r_v)^4]}. \quad (\text{A3})$$

We further approximate by assuming that the R^{-4} term is small compared to the first for the upper limit; that is, $1/4(a/R_{\text{CB}})^4 \ll 1.1R_{\text{CB}}$, which is a good approximation for $R_{\text{CB}} \geq 30 \mu\text{m}$, which is the case for all cases with drizzle greater than a few hundredths of a millimeter per day. Then (A2) yields an expression for the growth of the embryonic drizzle drops from cloud top to base:

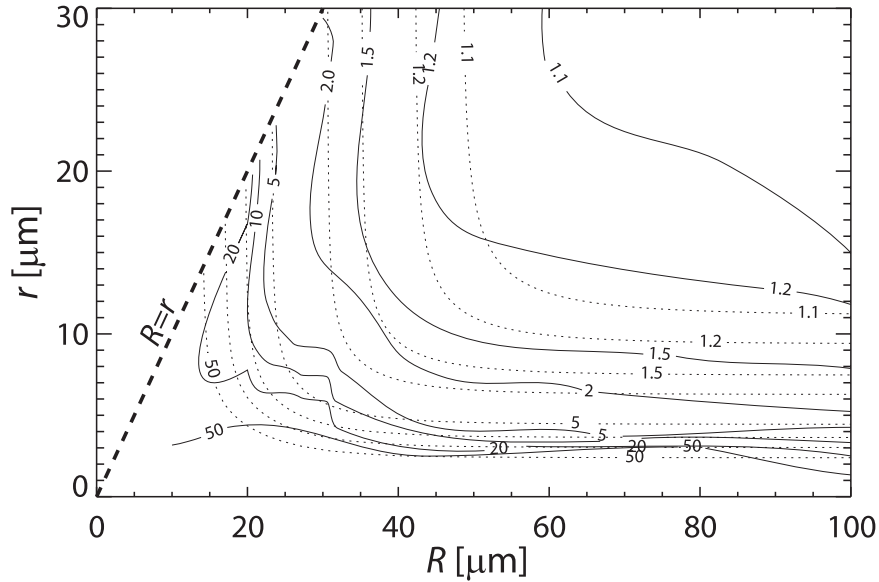


FIG. A1. Inverse collection efficiency $E^{-1}(R, r)$ from Hall (1980) (solid) and from (A2) (dotted). The dashed line represents $R = r$.

$$\Delta R = R_{\text{CB}} - R_{\text{emb}} = \frac{\eta \text{LWP}}{4\rho_w [1 + (b/r_v)^4]} - \frac{a^5}{4R_{\text{emb}}^4}. \quad (\text{A4})$$

Given the assumptions made regarding the cloud droplet size distribution—that is, model assumption 2 (see section 2a)—a simple parameterization for R_{emb} as a function of r_v is possible, namely $R_{\text{emb}} \approx c(r_v + d)$, with $c = 1.4$ and $d = 4.0 \mu\text{m}$ (note that the values of c and d will depend on the assumed precipitation embryo concentration N_D , here assumed to be 100 L^{-1} , and should be tuned if N_D is varied). Then (A4) becomes

$$\Delta R = R_{\text{CB}} - R_{\text{emb}} \approx \frac{\eta \text{LWP}}{4\rho_w [1 + (b/r_v)^4]} - \frac{a^5}{4c^4(r_v + d)^4}. \quad (\text{A5})$$

The precipitation rate at cloud base from the minimal model \tilde{P}_{CB} is then given by

$$\begin{aligned} \tilde{P}_{\text{CB}} &= \frac{4\pi\rho_w}{3} \alpha_T N_D R_{\text{CB}}^{3+\delta} \\ &= \frac{4\pi\rho_w}{3} \alpha_T N_D \left\{ c(r_v + d) + \frac{\eta \text{LWP}}{4\rho_w [1 + (b/r_v)^4]} - \frac{a^5}{4c^4(r_v + d)^4} \right\}^{3+\delta}. \end{aligned} \quad (\text{A7})$$

Equation (A7) expresses the cloud base precipitation rate as a function only of the cloud liquid water path and

the mean volume radius at cloud top (uniquely determined as a function of LWP and N_d for a given z_0). The first term in the parentheses represents a memory of the initial size of the embryonic drizzle drops. The second term represents the reservoir of available cloud water to be collected by the falling drizzle drops (with the denominator describing limits to their growth when the collected droplets are small and therefore collected inefficiently), and the third term is a suppression that represents inhibition by the limited *initial* size of the falling embryos themselves.

Figure A2 shows that the minimal model cloud base precipitation rate P_{CB} agrees very well with that from the full CC model and is able to demonstrate the increasing importance of LWP in determining the precipitation rate at low N_d and high LWP. Equation (A7) readily demonstrates sensitivity to both LWP and N_d consistent with observations in stratocumulus clouds (Pawlowska and Brenguier 2003; Comstock et al. 2004; vanZanten et al. 2005), but for deeper precipitating trade cumulus clouds (which typically have higher local LWP and low N_d) the sensitivity to LWP increases and that N_d decreases so that $\tilde{P}_{\text{CB}} \sim \text{LWP}^{3+\delta}$.

To further indicate the utility of the minimal model, Fig. A3 shows the relative importance of the three terms in (A7) superimposed on the precipitation rate from the CC model. As the precipitation rate increases, the term involving the accretion of cloud water becomes dominant. This also demonstrates that the cloud-top effective radius alone does not serve as a particularly useful predictor of the tendency to precipitation or of the rate

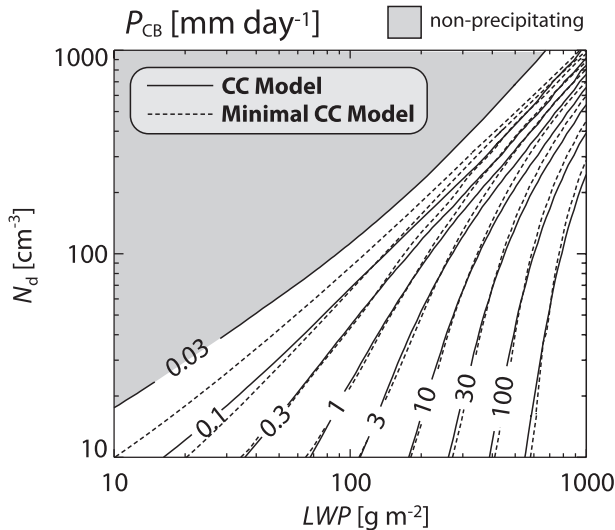


FIG. A2. Cloud-base precipitation rate P_{CB} as a function of cloud LWP and cloud droplet concentration N_d for the CC model (solid contours) and for the minimal CC model (dashed contours) described in the appendix. Model parameters are given in Table 1. The gray area indicates the parameter space where clouds are nonprecipitating (using a threshold of 0.03 mm day^{-1}).

that a cloud of a given thickness might produce. Only for the very smallest P_{CB} and for very low LWP are the precipitation isohyets even close to being parallel to the lines of constant effective radius.

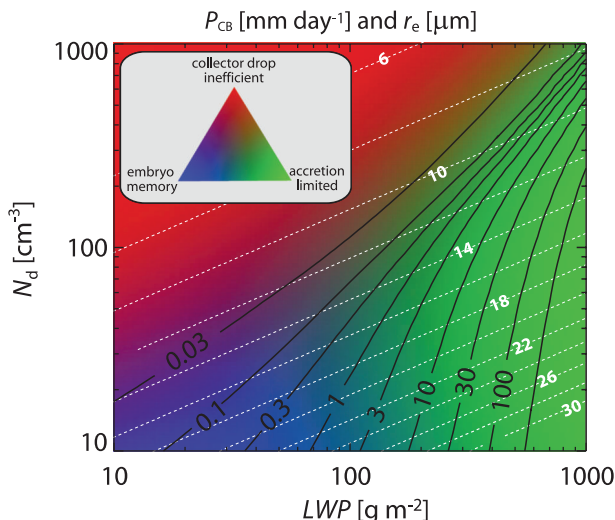


FIG. A3. Relative importance of the three terms (first term: embryo memory; second term: cloud liquid water available for accretion; third term: inhibition by the embryo collection inefficiency) in the minimal model expression for the P_{CB} [three terms in the curly parentheses in Eq. (A7)] as shown using the three primary colors (first term, blue; second term, green; third term, red). Also shown is P_{CB} for the CC model (solid contours) and the cloud-top effective radius r_e (dotted contours).

For these thicker clouds, where h is significantly larger than z_0 , LWP is approximately linearly dependent upon the cloud thickness. This is consistent with an observed lack of a trend in the liquid water profile with height for clouds thicker than about 1 km (Rauber et al. 2007). Thus, the CC model suggests that the precipitation rate in trade cumuli would scale with the cloud thickness to the fourth or fifth power, with a much weaker dependence on N_d , a result that is at least qualitatively consistent with recent large-eddy simulations (Stevens and Seifert 2008).

REFERENCES

- Ackerman, A. S., O. B. Toon, and P. V. Hobbs, 1993: Dissipation of marine stratiform clouds and collapse of the marine boundary layer due to the depletion of cloud condensation nuclei by clouds. *Science*, **262**, 226–229.
- Albrecht, B. A., 1989: Aerosols, cloud microphysics, and fractional cloudiness. *Science*, **245**, 1227–1230.
- Austin, P., Y. Wang, R. Pincus, and V. Kujala, 1995: Precipitation in stratocumulus clouds: Observations and modeling results. *J. Atmos. Sci.*, **52**, 2329–2352.
- Baker, M. B., 1993: Variability in concentrations of cloud condensation nuclei in the marine cloud-topped boundary layer. *Tellus*, **45B**, 458–472.
- Beheng, K. D., 1994: A parameterization of warm cloud microphysical conversion processes. *Atmos. Res.*, **33**, 193–206.
- Bohren, C. F., and D. R. Huffman, 1998: *Absorption and Scattering of Light by Small Particles*. Wiley-Interscience, 544 pp.
- Brenguier, J.-L., and R. Wood, 2009: Observational strategies from the micro- to mesoscale. *Clouds in the Perturbed Climate System: Their Relationship to Energy Balance, Atmospheric Dynamics, and Precipitation*, J. Heintzenberg and R. J. Charlson, Eds., Strüngmann Forum Report, The MIT Press, 487–510.
- Bretherton, C. S., J. R. McCaa, and H. Grenier, 2004: A new parameterization for shallow cumulus convection and its application to marine subtropical cloud-topped boundary layers. Part I: Description and 1D results. *Mon. Wea. Rev.*, **132**, 864–882.
- Byers, H. R., and R. K. Hall, 1955: A census of cumulus-cloud height versus precipitation in the vicinity of Puerto Rico during the winter and spring of 1953–1954. *J. Meteor.*, **12**, 176–178.
- Comstock, K., R. Wood, S. Yuter, and C. S. Bretherton, 2004: Reflectivity and rain rate in and below drizzling stratocumulus. *Quart. J. Roy. Meteor. Soc.*, **130**, 2891–2918.
- , C. S. Bretherton, and S. Yuter, 2005: Mesoscale variability and drizzle in southeast Pacific stratocumulus. *J. Atmos. Sci.*, **62**, 3792–3807.
- , S. E. Yuter, R. Wood, and C. S. Bretherton, 2007: The three-dimensional structure and kinematics of drizzling stratocumulus. *Mon. Wea. Rev.*, **135**, 3767–3784.
- Ferek, R. J., and Coauthors, 2000: Drizzle suppression in ship tracks. *J. Atmos. Sci.*, **57**, 2707–2728.
- Geoffroy, O., J. L. Brenguier, and I. Sandu, 2008: Relationship between drizzle rate, liquid water path and droplet concentration at the scale of a stratocumulus cloud system. *Atmos. Chem. Phys.*, **8**, 4641–4654.
- Ghan, S. J., and R. C. Easter, 1992: Computationally efficient approximations to stratiform cloud microphysics parameterization. *Mon. Wea. Rev.*, **120**, 1572–1582.

- Hall, W. D., 1980: A detailed microphysical model within a two-dimensional dynamic framework: Model description and preliminary results. *J. Atmos. Sci.*, **37**, 2486–2507.
- Haynes, J. M., T. S. L'Ecuyer, G. L. Stephens, S. D. Miller, C. Mitrescu, N. B. Wood, and S. Tanelli, 2009: Rainfall retrieval over the ocean with spaceborne W-band radar. *J. Geophys. Res.*, **114**, D00A22, doi:10.1029/2008JD009973.
- Hudson, J. G., and G. Svensson, 1995: Cloud microphysical relationships in California marine stratus. *J. Appl. Meteor.*, **34**, 2655–2666.
- Khairoutdinov, M., and Y. Kogan, 2000: A new cloud physics parameterization in a large-eddy simulation model of marine stratocumulus. *J. Atmos. Sci.*, **57**, 229–243.
- , and D. Randall, 2006: High-resolution simulation of shallow-to-deep convection transition over land. *J. Atmos. Sci.*, **63**, 3421–3436.
- Kuang, Z. M., and C. S. Bretherton, 2006: A mass-flux scheme view of a high-resolution simulation of a transition from shallow to deep cumulus convection. *J. Atmos. Sci.*, **63**, 1895–1909.
- Kubar, T. L., D. L. Hartmann, and R. Wood, 2009: Understanding the importance of microphysics and macrophysics for warm rain in marine low clouds. Part I: Satellite observations. *J. Atmos. Sci.*, **66**, 2953–2972.
- Levin, Z., and W. R. Cotton, 2008: *Aerosol Pollution Impact on Precipitation: A Scientific Review*. Springer, 386 pp.
- Lhermitte, R., 1990: Attenuation and scattering of millimeter wavelength radiation by clouds and precipitation. *J. Atmos. Oceanic Technol.*, **7**, 464–479.
- Liou, K. N., and S. C. Ou, 1989: The role of cloud microphysical processes in climate: An assessment from a one-dimensional perspective. *J. Geophys. Res.*, **94**, 8599–8607.
- Liu, Y., and P. H. Daum, 2004: On the parameterization of the autoconversion process. Part I: Analytical formulation of the Kessler-type parameterizations. *J. Atmos. Sci.*, **61**, 1539–1548.
- , —, and R. L. McGraw, 2005: Size truncation effect, threshold behavior, and a new type of autoconversion parameterization. *Geophys. Res. Lett.*, **32**, L11811, doi:10.1029/2005GL022636.
- Lohmann, U., and J. Feichter, 2005: Global indirect aerosol effects: A review. *Atmos. Chem. Phys.*, **5**, 715–737.
- Nicholls, S., 1989: The structure of radiatively driven convection in stratocumulus. *Quart. J. Roy. Meteor. Soc.*, **115**, 487–511.
- Nuijens, L., B. Stevens, and A. P. Siebesma, 2009: The environment of precipitating shallow convection. *J. Atmos. Sci.*, **66**, 1962–1976.
- Paluch, I. R., and D. H. Lenschow, 1991: Stratiform cloud formation in the marine boundary layer. *J. Atmos. Sci.*, **48**, 2141–2158.
- Pawlowska, H., and J.-L. Brenguier, 2003: An observational study of drizzle formation in stratocumulus clouds for general circulation model (GCM) parameterizations. *J. Geophys. Res.*, **108**, 8630, doi:10.1029/2002JD002679.
- Posselt, R., and U. Lohmann, 2008: Introduction of prognostic rain in ECHAM5: Design and single column model simulations. *Atmos. Chem. Phys.*, **8**, 2949–2963.
- Pruppacher, H. R., and J. D. Klett, 1997: *Microphysics of Clouds and Precipitation*. 2nd ed. Kluwer Academic, 976 pp.
- Rangno, A. L., and P. V. Hobbs, 2005: Microstructures and precipitation development in cumulus and small cumulonimbus clouds over the warm pool of the tropical Pacific Ocean. *Quart. J. Roy. Meteor. Soc.*, **131**, 639–673.
- Rauber, R. M., and Coauthors, 2007: Rain in shallow cumulus over the ocean—The RICO campaign. *Bull. Amer. Meteor. Soc.*, **88**, 1912–1928.
- Rogers, R. R., and M. K. Yau, 1989: *A Short Course in Cloud Physics*. Butterworth Heinemann, 290 pp.
- Savic-Jovicic, V., and B. Stevens, 2008: The structure and mesoscale organization of precipitating stratocumulus. *J. Atmos. Sci.*, **65**, 1587–1605.
- Seifert, A., and K. D. Beheng, 2001: A double-moment parameterization for simulating autoconversion, accretion and self-collection. *Atmos. Res.*, **59–60**, 265–281.
- Stevens, B., and A. Seifert, 2008: Understanding macrophysical outcomes of microphysical choices in simulations of shallow cumulus convection. *J. Meteor. Soc. Japan*, **86**, 143–162.
- , W. R. Cotton, G. Feingold, and C.-H. Moeng, 1998: Large-eddy simulations of strongly precipitating, shallow, stratocumulus-topped boundary layers. *J. Atmos. Sci.*, **55**, 3616–3638.
- , G. Vali, K. Comstock, R. Wood, M. vanZanten, P. H. Austin, C. S. Bretherton, and D. H. Lenschow, 2005: Pockets of open cells and drizzle in marine stratocumulus. *Bull. Amer. Meteor. Soc.*, **86**, 51–57.
- Tompkins, A. M., 2001: Organization of tropical convection in low vertical wind shears: The role of cold pools. *J. Atmos. Sci.*, **58**, 1650–1672.
- Tripoli, G. J., and W. R. Cotton, 1980: A numerical investigation of several factors contributing to the observed variable density of deep convection over south Florida. *J. Appl. Meteor.*, **19**, 1037–1063.
- vanZanten, M. C., B. Stevens, G. Vali, and D. Lenschow, 2005: Observations of drizzle in nocturnal marine stratocumulus. *J. Atmos. Sci.*, **62**, 88–106.
- Wang, H., and G. Feingold, 2009a: Modeling mesoscale cellular structures and drizzle in marine stratocumulus. Part I: Impact of drizzle on the formation and evolution of open cells. *J. Atmos. Sci.*, in press.
- , and —, 2009b: Modeling mesoscale cellular structures and drizzle in marine stratocumulus. Part II: The microphysics and dynamics of the boundary region between open and closed cells. *J. Atmos. Sci.*, in press.
- Wood, R., 2000: Parametrization of the effect of drizzle upon the droplet effective radius in stratocumulus clouds. *Quart. J. Roy. Meteor. Soc.*, **126**, 3309–3324.
- , 2005a: Drizzle in stratiform boundary layer clouds. Part I: Vertical and horizontal structure. *J. Atmos. Sci.*, **62**, 3011–3033.
- , 2005b: Drizzle in stratiform boundary layer clouds. Part II: Microphysical aspects. *J. Atmos. Sci.*, **62**, 3034–3050.
- , K. K. Comstock, C. S. Bretherton, C. Cornish, J. Tomlinson, D. R. Collins, and C. Fairall, 2008: Open cellular structure in marine stratocumulus sheets. *J. Geophys. Res.*, **113**, D12207, doi:10.1029/2007JD009371.
- Xue, H., G. Feingold, and B. Stevens, 2008: Aerosol effects on clouds, precipitation, and the organization of shallow cumulus convection. *J. Atmos. Sci.*, **65**, 392–406.